Intracellular XBP1-IL-24 axis dismantles cytotoxic unfolded protein response in the liver

Jianye Wang[1,7], Bian Hu[4,7], Zhicong Zhao[1], Haiyan Zhang[3], He Zhang[1,6], Zhenjun Zhao[1], Xiong Ma[3], Bin Shen[5], Beicheng Sun[2], Xingxu Huang[4]*, Jiajie Hou[1,2]* & Qiang Xia[1]*

[1]Department of Liver Surgery, Renji Hospital, School of Medicine, Shanghai Jiaotong University, Shanghai, China

[2]Department of Hepatobiliary Surgery, The Affiliated Drum Tower Hospital of Nanjing University Medical School, Nanjing, China

[3]Division of Gastroenterology and Hepatology, Key Laboratory of Gastroenterology and Hepatology, Ministry of Health; State Key Laboratory for Oncogenes and Related Genes, Renji Hospital; School of Medicine, Shanghai Jiao Tong University; and Shanghai Institute of Digestive Disease, Shanghai, China

[4]School of Life Science and Technology, ShanghaiTech University, Shanghai 201210, China

[5]State Key Laboratory of Reproductive Medicine, Department of Histology and Embryology, Nanjing Medical University, Nanjing, China

[6]Department of Surgery, The University of Hong Kong-Shenzhen Hospital, Shenzhen 518053, China

[7]These authors contributed equally

*__Correspondence__

Prof. Xingxu Huang: Phone: +86-21-20685028. Email: huangxx@shanghaitech.edu.cn

Prof. Jiajie Hou: Phone: + 86-25-83105892. Email: jethou0821@hotmail.com

Prof. Qiang Xia: Phone: +86-21-58752345. Email: xiaqiang@shsmu.edu.cn

Key words: IL-24, ER stress, Liver injury, XBP1, CHOP

Running Title: Intrinsic IL-24 inhibits liver injury

Numbers of Figures and tables: 7 main Figures, 0 table and 7 Expanded View Figures

Abbreviations: IL-24, interleukin 24; ER, endoplasmic reticulum; UPR, unfolded protein response; PERK, protein kinase RNA like ER kinase; IRE1, inositol-requiring enzyme 1; XBP1, X-box binding protein; ATF6, activating transcription factor 6; CHOP, transcription factor C/EBP homologous protein; GRP78, glucose-regulated protein 78; Tm, tunicamycin; ALT, alanine aminotransferase; AST, aspartate aminotransferase; CRISPR/Cas9, clustered regularly interspersed short palindromic repeats / CRISPR associated protein 9; ISRIB, inhibitor of the integrated stress response, AAV, adeno-associated virus; ALF, acute liver failure

Financial support statement

National Natural Science Foundation of China (81672801 to J.H., 81670598 to Q.X. and 81700498 to Haiyan Z.), Chen Guang Project in Shanghai Municipal Education Commission and Shanghai Education Development Foundation (15CG13 to J.H. and 17CG10 to Haiyan Z.) and National Key Research and Development Program of China (2016YFC0905901 to X.H.).

Abstract

Endoplasmic reticulum (ER) stress-associated cell death is prevalent in various liver diseases. However, the determinant mechanism how hepatocytes survive unresolved stress was still unclear. Interleukin-24 (IL-24) was previously found to promote ER stress-mediated cell death, and yet its expression and function in the liver remained elusive. Here we identified an anti-apoptotic role of IL-24, which transiently accumulated within ER-stressed hepatocytes in a X-box binding protein 1 (XBP1)-dependent manner. Disruption of IL-24 increased cell death in the CCL_4- or APAP-challenged mouse liver or Tm-treated hepatocytes. In contrast, pharmaceutical blockade of eukaryotic initiation factor 2α (eIF2α) or genetical ablation of C/EBP homologous protein (CHOP) restored hepatocyte function in the absence of IL-24. In a clinical setting, patients with acute liver failure manifested a profound decrease of hepatic IL-24 expression, which was associated with disease progression. In conclusion, intrinsic hepatocyte IL-24 maintains ER homeostasis by restricting the eIF2α-CHOP pathway-mediated stress signal, which might be exploited as a bio-index for prognosis or therapeutic intervention in patients with liver injury.

Introduction

The liver, one of the most vital organs in metabolic homeostasis, has a unique potential to fully recover from acute liver injury. Despite recent studies elucidating various molecular pathways involved in liver damage [1], a further understanding of the pivotal life-and-death decision mechanism is needed to improve current therapeutics. Endoplasmic reticulum (ER) content is rich in hepatocytes and participates in the processes of synthesizing, folding and trafficking of proteins [2, 3]. Environmental stimuli or nutrient fluctuations disrupt the ER protein-folding procedure, referred to as ER stress [4]. With an accumulation of misfolded proteins in ER lumen, the unfolded protein response (UPR), a collection of intracellular signal pathways, is activated to increase protein-folding capacity and reduce global protein synthesis. Once the molecular adaption fails in resolving the protein-folding defect, hepatocytes enter persistent ER stress, which results in apoptosis[5]. ER stress-related apoptosis has been found in fatty liver disease, viral hepatitis, and alcohol or drug induced liver injury [3, 6, 7]. The transcription factor C/EBP homologous protein (CHOP) mediates the most well-characterized pro-apoptotic pathway resulted from unresolved ER stress. CHOP induces the expression of pro-apoptotic BH3-only protein Bim, the cell surface death receptor TRAIL receptor 2, and inhibits Bcl2 transcription [8-11]. As previously reported, CHOP-deficient mice were protected from acetaminophen (APAP)-induced liver damage and conferred a survival advantage [12].

Interleukin-24 (IL-24) was first identified as a negative regulator in human melanocytes[13, 14]. As an IL-10 superfamily member, IL-24 has been reported to exert a bystander anti-cancer function, but has no deleterious effect toward non-cancerous cell [13, 15-17]. Like other secretory proteins, IL-24 precursor, which is 206 amino acids in length, translocates to the ER lumen before it proceeds to the secretory pathway. Independently of its cognate receptors, adenovirus-mediated IL-24 overexpression

in melanoma cells led to induction of apoptosis by interaction with glucose-regulated protein 78 (GRP78) and upregulation of GADD family genes, including CHOP [18, 19]. Nonetheless, little is known about IL-24 expression and its correlation with ER stress in non-cancerous cells. Interestingly, IL-24 production was elevated in diabetic pancreatic islets, where it induced beta cell ER stress and impaired glucose tolerance [20]. But it remains unclear whether IL-24 adapts ER homeostasis in epithelial cells.

Given the abundant IL-24 expression in the normal mouse or human liver detected in our preliminary experiments, the role of hepatocyte IL-24 in liver diseases has yet to be deciphered. To search for a possible link between IL-24 and ER stress within hepatocytes, we employed two mouse models characterizing IL-24 in the duration of acute liver injury. Unexpectedly, IL-24 deficiency did not alleviate liver damage but sensitized ER stressed hepatocytes to death. By monitoring tunicamycin (Tm)-stimulated mouse hepatocytes *in vitro* or manipulating the IL-24 level or UPR pathway *in vivo*, we further confirmed anti-apoptotic function of intracellular IL-24. Indeed, we revealed that hepatocyte IL-24 governs the intrinsic adaption to ER stress by control of PERK-eIF2α-CHOP pathway. Collectively, these results highlight profound implications for understanding hepatocyte ER homeostasis and identify IL-24 as a critical anti-stress factor in the liver.

Results

Hepatocyte IL-24 transiently increases during ER stress-related acute liver injury.

Firstly, we detected the expression of IL-24 among different organs in normal wild type (WT) mice and found it was most highly expressed in the liver (Expanded View Fig. 1A). To explore whether liver IL-24 is linked to ER stress, we treated WT mice with a single dose of CCl_4 (2ml/kg) as reported previously[19]. Serum levels of alanine aminotransferase (ALT) and aspartate aminotransferase (AST) were markedly elevated and peaked at 48 h post treatment, then returned to baseline at 72 h time point

(Expanded View Fig. 1B). In context, exposure to CCL_4 unaffected the ER chaperon GRP78 but tremendously evoked CHOP expression in the liver (Fig. 1A&B). Noticeably, IL-24 mRNA level was transiently increased at 24 h, then decreased and reverted to normal level 72 h post CCL_4 administration. A same trend was observed in IL-24 protein level (Fig. 1A). Regarding the potential inflammatory responses caused by CCL_4, we also measured the serum IL-24 protein level. Nonetheless, CCL_4-treated mice exhibited undetectable serum IL-24, which was comparable to that in none-treated WT or IL-24 KO mice (data not show). Given the fact that hepatocytes take up the majority of hepatic cells, we asked whether the fluctuation of IL-24 expression was occurred in ER stressed-hepatocytes. To answer this question, we investigated IL-24 expression in murine hepatocyte cell line AML12 in the presence of an ER stress inducer Tm. Consistent with the *in vivo* observation, a transient increase of IL-24 level was recapitulated in AML12 upon ER stress, as accompanied by accumulating CHOP expression. These results suggested a potential role of non-secreted IL-24 and prompted us to understand how IL-24 was involved in hepatocyte ER stress.

The transcription factors activating transcription factor 4 (ATF4), ATF6, sliced X-box binding protein 1 (sXBP1) and CHOP regulate UPR-related gene expression[5]. Like CHOP, other three molecules were also upregulated in the CCL_4-exposed mouse liver or ER stressed-AML12 cells, among which sXBP1 was the first to peak (Expanded View Fig. 1C&D). Intriguingly, the murine *Il24* promoter harbors conserved binding motifs for ATF6/XBP1 and CHOP [21, 22](Expanded View Fig. 2A). To explore how IL-24 expression was affected in response to ER stress, we transfected AML12 cells with small interfering RNAs (siRNAs) targeting ATF4, ATF6, XBP1 and CHOP prior to Tm stimulation. IL-24 mRNA levels in these siRNA-expressing cells all decreased as compare to the negative control (NC) (Expanded View Fig. 2B), suggesting a regulatory relation between hepatocyte IL-24 and UPR

pathways. Importantly, siXBP1 most significantly inhibited IL-24 mRNA level and blocked its upregulation in response to ER stress. Silencing of XBP1 (but not CHOP or ATF6) repressed IL-24 protein level as well as *Il24 promoter* activity in Tm-stimulated AML12 cells (Fig. 1E&F and Expanded View Fig. 2C). Furthermore, we isolated primary hepatocytes from conditional XBP1 KO ($Xbp1^{f/w}$;Alb^{Cre}) mice. XBP1 depletion unaffected cell viability under ER stress, but reduced IL-24 in both mRNA and protein levels (Expanded View Fig. 2D-F).

Hepatocyte IL-24 deficiency promotes ER stress-related liver injury.

To further dissect the underlying impact of IL-24 fluctuation, IL-24 KO mice, in which 3306 bp of IL-24 allele was depleted, were subjected to CCL_4-induced liver injury. In comparison to the WT mice, IL-24-null littermates were more susceptible to CCL_4-induced liver injury, exhibiting a relatively higher ALT and AST level and a lower survival rate (Fig. 2A&B). The exacerbated liver damage in IL-24-null mice was visualized by hematoxylin and eosin (H&E). Meanwhile, a marked increase in the percentage of terminal deoxynucleotidyl transferase dUTP nick end labeling (TUNEL)-positive hepatocyte was observed in IL-24-null mice with respect to WT mice (Fig. 2C&D). Besides, proliferating cell nuclear antigen (PCNA) staining showed an increase of cell proliferation in IL-24 KO mice (Expanded View Fig. 3A), possibly due to compensatory liver regeneration. We then checked the inflammatory status and detected higher IL1A and IL6 and lower TNFA mRNA expression in the IL-24-deficient mouse liver (Expanded View Fig. 3B). Overdose of APAP, an analgesic and antipyretic drug, is the leading cause of drug-induced acute liver injury [23]. Accordingly, we subjected IL-24-null mice to oral administration of APAP, which was evident for inducing ER stress-related liver damage [12]. In context, worse liver function and survival rate and extensive hepatocyte death were manifested in IL-24-deficient group (Expanded View Fig. 3C-E). Given the possibility that the extracellular IL-24 might be implicated in liver

injury, we treated WT mice with recombinant IL-24 (rIL-24) one hour before administration with CCl_4. Nonetheless, the levels of transaminases, percentages of hepatocyte death and expression of P-PERK and CHOP showed no statistical differences between vehicle and cytokine-treated mice (Expanded View Fig. 4A-C).

To obtain a closer insight into the intrinsic IL-24 function, we genetically depleted IL-24 in AML12 cells by using clustered regularly interspersed short palindromic repeats (CRISPR) / CRISPR associated protein 9 (Cas9) strategy and treated with Tm to mimic the pathological process *in vivo*. Cell Counting Kit-8 (CCK8) assays indicated that loss of intrinsic IL-24 impaired cell viability. Reciprocally, overexpression of IL-24 in AML12 benefited cell survival upon ER stress (Fig. 2F). Furthermore, annexin-V and propidium iodide staining showed that IL-24 attenuated late phase of apoptosis (Expanded View Fig. 5A&B). Together, these results suggested that hepatocyte IL-24 plays a fundamental role in protecting ER stress-mediated cell death.

Hepatocyte IL-24 deficiency activates PERK-eIF2α-CHOP pathway.

To understand the mechanism behind hepatocyte stress, we assessed CHOP expression in both two acute liver injury models and Tm-exposed AML12 cells. Remarkably, loss of IL-24 in the mouse liver or hepatocytes unleashed CHOP expression, while introduction of IL-24 into AML12 efficiently diminished CHOP level (Fig. 3A&B and Expanded View Fig. 6A&B&C). In line with these findings, IL-24 depletion upregulated the expression of pro-apoptotic factors such as Bim and TRIB3, and yet downregulated anti-apoptotic molecule Bcl2 (Expanded View Fig. 6D). To analyze how IL-24 was linked to ER stress, we further examined the UPR branches in the upstream of CHOP. Unexpectedly, either IRE1α phosphorylation or ATF6 expression appeared no difference between WT and IL-24 KO mice (Expanded View Fig. 6E). Noticeably, phosphorylation of PERK was selectively upregulated in the IL-

177 24-deficient mouse liver or AML12 cells, and conversely downregulated upon IL-24 overexpression
178 (Fig. 3A&B and Expanded View Fig. 6A). Accordingly, we evaluated the downstream molecules of
179 PERK and found IL-24 deficiency robustly reinforced phosphorylation of eIF2α and expression of ATF4
180 and GADD34 in the stressed liver or AML12 cells, while overexpression of IL-24 in AML12 cells inhibited
181 these molecules (Fig. 3A-E and Expanded View Fig. 6A-C). Immunohistochemical staining further
182 confirmed higher levels of P-eIF2α and CHOP in IL-24-deficient liver (Fig. 3C). In aligned with these
183 results, primary mouse hepatocytes isolated from IL-24-null mice manifested excessive activation of
184 PERK-CHOP signal upon Tm-induced unresolved ER stress (Fig. 3F). Similarly, we also confirmed the
185 activation of PERK-CHOP pathway in IL-24-deficient cells under *in vitro* CCL_4 treatment (Expanded
186 View Fig. 6F).

187 **Hepatocyte IL-24 selectively limits CHOP-mediated death signal.**

188 To explore whether CHOP is indispensable for IL-24 deficiency-related hepatocyte damage, we utilized
189 siRNA targeting CHOP (siCHOP) to comprehend its executive role in ER-stressed hepatocytes.
190 Administration of siCHOP to AML12 cells offset the marginal cell death caused by IL-24 depletion (Fig.
191 4A). In addition, we crossed IL-24-null mice with a CHOP-null strain to generate a double knockout
192 (DKO) strain. In contrast to IL-24 KO counterparts, both CHOP KO and DKO mice rejected to CCL_4-
193 induced liver injury (Fig. 4B). As evident in histological staining, disruption of CHOP eliminated
194 hepatocyte death in IL-24 KO mice (Fig. 4C). Therefore, these results suggest that IL-24 deficiency
195 promotes hepatocyte death dependently on CHOP in the context of unresolved ER stress.

196 To better understand the intrahepatic function of IL-24, we treated the IL-24 null mice with IL-24-
197 expressing adeno-associated viral (AAV) particles 8 weeks prior to CCL_4 administration. As shown in
198 Fig. 4D&E, re-expression of IL-24 in the liver markedly reduced the levels of serum transferases and

199 P-PERK, P-eIF2α and CHOP.

200 **Hepatocyte IL-24 attenuates liver damage by restricting the PERK-eIF2α branch.**

201 To ascertain the importance of PERK-eIF2α UPR branch, we built on an observation made with the
202 inhibitor of the integrated stress response (ISRIB), which specifically blocks PERK-eIF2α signaling but
203 unaffects ATF6 or inositol-requiring enzyme 1 (IRE1α) pathway[24]. Strikingly, pretreating AML12 with
204 ISRIB compensated the viability loss for the lack of IL-24 but did not change the viability of WT cells
205 (Fig. 5A). Next, we treated IL-24-null mice with vehicle or ISRIB one hour prior to CCL_4 administration.
206 As indicated by serum aminotransferases, ISRIB reversed the deterioration of liver damage in IL-24-
207 null mice but showed no profound impact on WT mice (Fig. 5B). H&E and TUNEL staining visualized
208 an amelioration in hepatocyte death intensified by IL-24 depletion (Fig. 5C), which could be explained
209 by the reduction of CHOP expression after ISRIB treatment (Fig. 5D).

210 It is known that the ER protein chaperon GRP78 binds to the cytoplasmic and ER luminal domains of
211 PERK to prevent its activation[25]. Accordingly, we asked whether hepatocyte IL-24 affected the
212 interaction between GRP78 and PERK. By performing immunoprecipitation, we pulled down GRP78 in
213 AML12 cells and detected a significant binding of PERK after 6 h of Tm stimulation. In concert with the
214 UPR degrees, its association with PERK was significantly enhanced in IL-24-deficient cells and was
215 weakened in IL-24-overexpressed cells (Fig. 5E and Expanded View Fig. 7A). To obtain a functional
216 relevance *in vivo*, we replenished chaperon expression in the mouse liver by intravenous injection of
217 GRP78-expressing AAV. As shown in Fig. 5F and Expanded View Fig. 7B&C, overexpression of GRP78
218 strongly mitigated liver damage and PERK-CHOP activation in the CCL_4-treated IL-24-null mice.

219 **Hepatocyte IL-24 predicts prognosis for patients with acute liver injury.**

220 To examine the biological significance of IL-24 in clinical situations, we collected liver tissue and serum

221 samples from 9 heathy donors, 9 patients with liver cirrhosis and 22 patients with acute liver failure
222 (ALF). Serum IL-24 levels in both two groups of liver injury patients were as low as that in heathy donors
223 (data not shown), which was aligned with what we found in CCL_4-induced liver injury mouse models.
224 Nonetheless, immunohistochemistry, immunoblots and qRT-PCR indicated that IL-24 expression was
225 reduced in patients with liver cirrhosis and even lower in those with ALF (Fig. 6A-C&F), whereas CHOP
226 expression was concomitantly escalated in cirrhosis and ALF patients (Fig. 6A&F), suggestive of a
227 strong correlation between IL-24 expression and hepatocyte stress. In a further analysis of ALF patients,
228 we obtained the individual liver function test before liver transplant and found IL-24 expression in
229 hepatocytes was negatively related to serum ALT level as well as liver CHOP expression (Fig. 6D&E).
230 Taken together, hepatocyte IL-24 may function as a prognosis predictor for patients with acute liver
231 injury.

232 **Discussion**

233 UPR is executed through three ER transmembrane stress sensors: IRE1α, PERK and activating
234 transcription factor 6 (ATF6)[5]. Activated IRE1α splices XBP1 mRNA, which encodes transcription
235 factor to increase the protein-folding capacity and degrade misfolded proteins. While IRE1α engages
236 STAT3 pathway to promote liver regeneration upon liver injury [26], XBP1 switches pro-survival to pro-
237 apoptotic signal cascades through multiple gene regulation [27, 28]. It has been reported that ATF6
238 exerts a pro-inflammatory effect on ischemia-reperfusion liver injury [29]. PERK antagonizes UPR by
239 reducing the flux of protein translocating and phosphorylating eIF2α, a pervasive translation initiation
240 factor, which inhibits ribosome assembly and translation. However, eIF2α selectively upregulates the
241 transcription factor ATF4 and its downstream target CHOP. Sustained ER stress engages CHOP to
242 enhance UPR and inflammation signaling and lead to apoptosis [22, 30]. The mouse models in our

243 study manifested activation of three UPR sensors and CHOP. The latter was also found to be
244 upregulated in human cirrhosis and ALF patients. Given the recovery of liver function in most cases,
245 we hypothesized an unknown machinery restoring hepatocyte ER homeostasis.

246 IL-24 has been reported to cause ER stress-mediated apoptosis through a secretion-independent
247 manner [19]. Unexpectedly, we detected abundant IL-24 expression in the mouse or human liver under
248 normal condition. In the CCL_4 model, hepatocyte IL-24 increases instantaneously and then returns to
249 baseline as the liver function recovers. Nonetheless, serum IL-24 was undetectable in CCL_4-treated
250 mice and human cirrhosis and ALF patients, excluding its engagement as a “hepatokine” in UPR
251 condition. Importantly, targeting ER stress-related transcription factors (ATF4, ATF6, XBP1 and CHOP)
252 significantly reduced the mRNA level of hepatocyte IL-24. However, only silencing of XBP1 deprived
253 IL-24 expression under either normal or deleterious circumstance. This reflects a physiological function
254 of hepatic XBP1 and also raises a possibility that intrinsic IL-24 may regulate stress signals.

255 Since adenovirus-mediated overexpression causes protein synthesis overload and induces potential
256 UPR, we employed gene knockout mice to improve our understanding of cytosolic IL-24 in ER stress
257 and liver damage. Remarkably, we found IL-24-null mice were more sensitive to CCL_4-induced liver
258 injury than WT counterparts. While either ATF6 expression or IRE1α phosphorylation was unaffected,
259 P-PERK, P-eIF2α, CHOP and GADD34 exhibited excessive expression in the IL-24-deficient mouse
260 liver. In addition, our results showed elevated levels of Bim and TRIB3 and a reduced level of Bcl2 in
261 IL-24-null mice, which might be a consequence of CHOP activation [3, 11]. Effects of hepatocyte IL-24
262 on PERK-eIF2α-CHOP branch and cell death were corroborated by depleting or introducing IL-24 in
263 AML12 cells. Furthermore, knocking out CHOP in IL-24-null mice or knocking down CHOP in IL-24-null
264 AML12 protected ER stress-associated hepatocyte damage. It has been reported that eIF2α

phosphorylation acts as a central event sensitizing stressed cells to death [12, 27, 29]. Accordingly, we found that the extensive liver damage in IL-24-null mice could be alleviated by administration of ISRIB, which selectively reverses the effects of eIF2α phosphorylation [24]. Clinically, we observed a concomitant downregulation of IL-24 and upregulation of CHOP in the cirrhosis and ALF tissues as compared with the healthy liver. Taken together, these findings demonstrated the protective role of IL-24 in resolving hepatocyte ER stress is implemented by perturbation of PERK-eIF2α-CHOP pathway.

As one of the most important ER chaperons, GRP78 is essential in conjunction with misfolded proteins and is important for maintaining ER homeostasis [8, 31]. Given the reinforced ER stress in IL-24-null hepatocytes, GRP78 conserved its affinity to combine and sequester overreacted PERK. Despite this, redundant PERK phosphorylated itself and triggered the downstream signaling. Previous study indicated that *in vivo* overexpression of GRP78 using an adenovirus vector could attenuate ER stress-associated liver steatosis [32]. In this study, introduction of GRP78 in the IL-24-deficient mouse liver by AAV infection attenuated PERK-facilitated hepatocyte stress. This may provide a potential therapeutic opportunity for UPR-related human liver diseases, especially those with low hepatocyte IL-24 expression.

To our knowledge, a variety of cytokines, including those expressed or secreted by hepatocytes, evoke inflammatory responses and promote cell death in liver diseases. In a diet-induced steatohepatitis mouse model, hepatocyte IL-1α was found to be upregulated in response to ER stress, which in turn enhanced CHOP expression; IL-1α released from necrotic hepatocytes accelerates steatohepatitis via induction of inflammatory cytokines [33, 34]. In lipopolysaccharide (LPS)-induced liver injury, hepatocyte-derived IL-7 augmented CD8+ T cell cytotoxic activity and promoted the development of autoimmune diseases [35]. In the present study, we showed that intracellular IL-24

uniquely benefited hepatocyte ER homeostasis, exerting an anti-inflammatory effect. However, it has not been defined whether hepatocyte can secrete IL-24 under pathological conditions and how it affects hepatocytes or immune cell populations in an autocrine or paracrine fashion.

Conclusively, we uncovered that cytosolic IL-24 is critical for protecting ER stressed-hepatocytes from death, which may be a good diagnostic and therapeutic target for clinical liver diseases.

Materials and Methods

Patients. Cirrhosis and liver failure tissues were collected from liver transplant recipients treated in Department of Liver Surgery, Renji Hospital, School of Medicine, Shanghai Jiaotong University. Normal liver tissues were collected from the healthy transplant donors through liver biopsy. All samples were collected with informed consent, and the experiments were approved by the ethical review committee of the World Health Organization Collaborating Center for Research in Human Production (authorized by the Shanghai Municipal Government).

Mice. All mice used in this study were in C57BL/6J background. IL-24 knockout (KO) mice were generated in ShanghaiTech University. The targeted Embryonic stem (ES) cells were ordered from The Knockout Mouse Project (KOMP) Repository, in which the insertion of Velocigene cassette ZEN-Ub1 created a deletion of size 3306 bp between positions 132779010-132782315 of Chromosome 1 (Genome Build37). These ES cells were injected into albino C57BL/6J blastocysts and the following inbred strain was generated by backcrossing breeding. The following PCR primers were used to identify WT (571 bp) and KO (338 bp) alleles: 5'- GTACCCACTCCAATGCATACATT -3', 5'-GCTCATCCAGGATGAAGCTACAC -3', and 5'-GAAACCAGGCAAATCTCCACTCC -3'. The CHOP KO mice and Alb^{Cre} transgenic mice were purchased from Jackson Laboratories. We crossed the CHOP KO and IL-24 KO strains to produce the double knockout (DKO) strain. The $Xbp1^{F/F}$ strain, a gift from

Dana Farber Cancer Institute, USA, was previously described [36]. Mice devoid of XBP1 selectively in hepatocytes were generated by breeding the $Xbp1^{F/F}$ mice with Alb^{Cre} strain. For acute liver injury model, CCL_4 dissolved in olive oil was injected intraperitoneally into 8-week-old female mice at a dose of 2 ml/kg [26]. Besides, mice were fasted overnight and administered 500 mg/kg APAP (Sigma) by oral gavage [12]. In some settings, mice were intraperitoneally injected with 0.25 mg/kg ISRIB (Selleck) or recombinant IL-24 (R&D) at a dose of 5 μg per mouse one hour prior to CCL_4 administration. All mice were maintained under specific pathogen-free (SPF) conditions, on a 12 h light-dark cycle. All mouse experiments were approved by the Shanghai Administrative Committee for Laboratory Animals.

Isolation of primary mouse hepatocytes and cell cultures. The mouse liver was perfused with an EGTA-buffer (37°C) at a constant flow of 5 ml/min for 8 minutes via the hepatic portal vein. Next, a secondary perfusion with a solution of collagenase I (Sigma-Aldrich) for 10 minutes (2 ml/min) is required for a completely digestion. The liver was disrupted gently to release hepatocytes into a suspension buffer. Subsequently, the liver capsule was filtered through a 70-μm cell strainer and the primary hepatocytes were collected after three cycles of centrifugations at 400 rpm for 5 min at 4°C. A suspension of 1×10^6 cells/mL was successively seeded in culture plates. Murine hepatocyte cell line AML12 was from The First Affiliated Hospital of Nanjing Medical University. Primary hepatocytes and AML12 cells were cultured in William's E Medium (Gibco) supplemented with 1X insulin-transferrin-selenium supplement (Gibco), 1X sodium pyruvate (Gibco), 40 ng/ml dexamethasone (Sigma-Aldrich) and 10% FBS (Gibco), incubated at 37 °C and 5% CO_2, and were tested for mycoplasma contamination once every three months. In some settings, cells were treated with 5 μg/ml Tm (Sangon Biotech) or 200 nM ISRIB (Selleck).

siRNA, sgRNA and gene transfection. The siRNAs were transiently transfected into AML12 cells by

using Lipofectamine RNAiMAX (Invitrogen) following manufacturer's instructions. A non-target siRNA was used as negative control. The siRNA sequences are listed as below: mouse XBP1, CCAAGCUGGAAGCCAUUAATT; mouse CHOP, CCAGAUUCCAGUCAGAGUUTT; mouse ATF4, CUCCCAGAAAGUUUAAUAATT; mouse ATF6, GCAGUCGAUUAUCAGCAUATT. Stable knockout of IL24 in AML12 cells was generated by lentiviral-based delivery of sgRNA/cas9 components. Briefly, sgRNA targeting the exonic region of murine *Il24* gene (5′-GAAGGATTAGGCTCAGGCAG-3′) were subcloned into the lentiviral vector GV393 (U6-sgRNA-EF1a-Cas9-FLAG-P2A-EGFP) (Genechem, China), while a non-target sgRNA (5′-CGCTTCCGCGGCCCGTTCAA-3′) was used as a negative control. IL-24-overexpression construct was generated by subcloning PCR-amplified full-length cDNA (NM_053095) into a GV358 (Ubi-MCS-Flag-SV40-EGFP-IRES-puromycin) lentiviral vector (Shanghai Genechem). An empty vector was used as a negative control. Viral particles were packaged in 293T cell and used to infect AML12 cells in the presence of 8 μg/ml polybrene followed by puromycin selection.

Recombinant AAV construction and In vivo transduction. GRP78-overexpression construct was generated by subcloning PCR-amplified full-length *Il24* (NM_053095) or *Hspa5* (NM_022310) cDNA into a GV461 (CMV-betaGlobin-MCS-SV40 PolyA) AAV vector (Shanghai Genechem). An empty vector was used as a negative control. IL24 KO mice of 5 weeks were intravenously injected with 2 x 10^{11} vector-genome (vg) AAV 8 weeks prior to CCL_4 administration.

Immunohistochemistry and Immunofluorescence. Immunohistochemistry for target molecules was performed on serial sections from human or mouse liver tissues. Sections were deparaffinized, subjected to antigen retrieval, and incubated with primary antibodies against IL-24 (Abcam, ab115207), P-eIF2a (Huabio, ET1603-14) and CHOP (Huabio, ET1703-05). All responses were followed by staining with the corresponding HRP-conjugated secondary antibody (Jackson Immuno Research Laboratories).

353 The stained slides were assessed with integrated optical density (IOD) using ImageJ software. The
354 apoptotic cells were defined by using In Situ Cell Death Detection Kit (Roche) following manufacturer's
355 protocol and quantified by calculating positively stained cells in at least five randomly chosen HPFs of
356 each slide.

357 **Immunoprecipitation.** Cell samples were collected and lysed in IP lysis buffer (Thermo Fisher)
358 containing protease inhibitor cocktail (Merck Millipore) for 30 minutes. After an insoluble product-clear
359 step by full speed centrifuge, the supernatant was harvest and incubated with anti-GRP78 (Abcam,
360 ab21685) antibody and protein A beads (Thermo Fisher) at 4 °C overnight. The beads were collected
361 and washed extensively, and the immuno-complex was eluted with western blot loading buffer.

362 **Western blot.** Cell or tissue lysates were separated on 6-8% polyacrylamide-SDS gels and transferred
363 to a nitrocellulose membrane using transfer buffer (25 mM Tris, 192 mM glycine and 10% methanol).
364 The blots were blocked with 5% non-fat milk in PBS containing 0.05% Tween-20 for 1 h and then probed
365 overnight at 4°C in PBST with primary antibodies. Next, the blots were incubated with a secondary
366 antibody conjugated to horseradish peroxidase (HRP) (1:5,000, Jackson Immuno Research
367 Laboratories) and detected with a ChemiDoc XRS system (Bio-Rad). Primary antibodies used in
368 western blot are listed below: anti-Flag (14793S), anti-P-PERK (3179S), anti-ATF4 (11815S) and anti-
369 CHOP (2895S) were from Cell Signal Technology, anti-human IL-24 (ab115207), anti-P-eIF2a
370 (ab32157) and anti-GRP78 (ab21685) were from Abcam, anti-mouse IL-24 (MAB2786) was from R&D
371 Systems, anti-PERK (sc-377400) was from Santa Cruz.

372 **Quantitative PCR (qPCR).** Total RNA samples used for RT-qPCR were isolated by using an RNeasy
373 kit (BioTeke) with an additional on-column DNase-I digestion step. Total RNA or purified mRNA was
374 reverse transcribed with PrimeScript™ RT Master Mix (Takara) using Oligo dT primers to obtain

complementary DNA. qPCR was carried out by using SYBR Premix Ex Taq II (Takara). β-actin was used as an internal control. The primers used in this study are: mouse GRP78(F:5'-TCATCGGACGCACTTGGAA -3';R:5'- CAACCACCTTGAATGGCAAGA -3'); mouse CHOP(F:5'-CTGGAAGCCTGGTATGAGGAT-3';R:5'- CAGGGTCAAGAGTAGTGAAGGT -3') ; mouse ATF4(F:5' -CTCTTGACCACGTTGGATGAC - 3'; R: 5' - CAACTTCACTGCCTAGCTCTAAA -3') ; mouse IL-24 (F:5'- GAGCCTGCCCAACTTTTTGTG -3';R:5'- TGTAGTCCCCAACTCATCTGTG -3'); mouse sXBP1 (F: 5'- CTGAGTCCGAATCAGGTGCAG -3'; R: 5'- GTCCATGGGAAGATGTTCTGG - 3'); mouse ATF6 (F: 5'- TCGCCTTTTAGTCCGGTTCTT -3'; R: 5'- GGCTCCATAGGTCTGACTCC - 3'); mouse GADD34 (F: 5'- GAGGGACGCCCACAACTTC -3'; R: 5'- TTACCAGAGACAGGGGTAGGT - 3'); mouse IL6 (F: 5'- TAGTCCTTCCTACCCCAATTTCC -3'; R: 5'- TTGGTCCTTAGCCACTCCTTC - 3'); mouse IL1A (F: 5'- CGAAGACTACAGTTCTGCCATT -3'; R: 5'- GACGTTTCAGAGGTTCTCAGAG - 3'); mouse Bim (F: 5'- GACAGAACCGCAAGGTAATCC -3'; R: 5'- ACTTGTCACAACTCATGGGTG - 3'); mouse TRIB3 (F: 5'- GCAAAGCGGCTGATGTCTG -3'; R: 5'-AGAGTCGTGGAATGGGTATCTG - 3'); mouse Bcl2 (F: 5'-ATGCCTTTGTGGAACTATATGGC -3'; R: 5'- GGTATGCACCCAGAGTGATGC - 3'); mouse TNFA (F: 5'- CTCTTCTGTCTACTGAACTTC -3'; R: 5'- CTCCTGGTATGAGATAGCAA - 3'); mouse β-actin (F:5'-ACCCACACTGTGCCCATCTAC -3';R:5'- AGCCAAGTCCAGACGCAGG -3'); human IL-24(F:5'-CACACAGGCGGTTTCTGCTAT-3'; R:5'- TCCAACTGTTTGAATGCTCTCC -3'); human β-actin (F: 5'-GGGAAATCGTGCGTGACATTAAG -3'; R: 5'- TGTGTTGGCGTACAGGTCTTTG - 3').

Dual luciferase assay. A DNA fragment of *Il24* (-1036 ~ -598 bp in the upstream of transcription start site) was subcloned into a luciferase reporter vector pGL4 (Promega). AML12 cells were cultured in 24-well plates for 24 hours, then transfected with siRNAs. The cells were co-transfected with luciferase reporter plasmid and renilla luciferase plasmid (an internal control) at a ratio of 10:1. Twenty-four hours

later, cells were treated with Tm (5 μg/ml). Cells from each independent well were harvested and detected by Dual-Luciferase Reporter Assay System (Promega) at indicated time. Get the relative light unit (RLU) by normalizing to renilla luminescence activities.

Apoptosis analysis. AML12 cells were stimulated by Tm, and 1~5x10^5 cells were collected by centrifugation. The cells were resuspended with the 1x Binding Buffer and incubated with 5μL FITC-conjugated annexin V Annexin FITC (BD Biosciences, USA) and 5μL PI (BD Biosciences, USA) to each tube according to the experimental protocol. Then samples were analyzed by fluorescence-activated cell sorter (FACS).

Statistical analysis At least three biological replicates were used in each experiment unless otherwise stated. Data were analyzed with GrapPad Prism 7 and were presented as the mean ± standard error of the mean (SEM). Two-tailed Student's t-tests were performed to assess the statistical significance of differences between groups. Pearson correlation coefficients (*r*) were calculated to assess correlation and statistical significance was assessed by a two-tailed t-test of $r = 0$.

Expanded View for this article is available online

Acknowledgements

We thank all patients and donors for participating in this study. We thank Ms Jiaxin Li (Renji Hospital, Shanghai, China) for helping with clinical sample collection, Dr. Indrajit Das (QIMR Berghofer Medical Institute, QLD, Australia) for the advice on ER stress antagonism, and Dr. Laurie H. Glimcher (Dana-Farber Cancer Institute, MA, USA) for providing $Xbp1^{F/F}$ mice as a kind gift. This study was supported by National Natural Science Foundation of China (81672801 to JH, 81670598 to QX and 81700498 to Haiyan Z), Chen Guang Project in Shanghai Municipal Education Commission and Shanghai Education Development Foundation (15CG13 to JH and 17CG20 to Haiyan Z) and National Key Research and

Development Program of China (2016YFC0905901 to XH).

Author contributions

J.H., X.H. and Q.X. conceived and designed the project, analysed and interpreted results, obtained funding and wrote the manuscript; J.W. and B.H. designed and performed experiments, analysed and interpreted results and wrote the manuscript; He Zhang, Zhenjun Zhao, Zhicong Zhao contributed to design and conduction of experiments and to analysis and interpretation of data; Haiyan Zhang, XM, Bin Shen and Beicheng Sun contributed to conception of research.

Conflict of interest: The authors declare no conflict of interest.

References

1. Schwabe RF, Luedde T (2018) Apoptosis and necroptosis in the liver: a matter of life and death. *Nat Rev Gastroenterol Hepatol*
2. Dara L, Ji C, Kaplowitz N (2011) The contribution of endoplasmic reticulum stress to liver diseases. *Hepatology* **53**: 1752-63
3. Malhi H, Kaufman RJ (2011) Endoplasmic reticulum stress in liver disease. *J Hepatol* **54**: 795-809
4. Hiramatsu N, Chiang W-C, Kurt TD, Sigurdson CJ, Lin JH (2015) Multiple Mechanisms of Unfolded Protein Response-Induced Cell Death. *Am J Pathol* **185**: 1800-8
5. Walter P, Ron D (2011) The unfolded protein response: from stress pathway to homeostatic regulation. *Science* **334**: 1081-6
6. He C, Qiu Y, Han P, Chen Y, Zhang L, Yuan Q, Zhang T, Cheng T, Yuan L, Huang C*, et al.* (2018) ER stress regulating protein phosphatase 2A-B56gamma, targeted by hepatitis B virus X protein, induces cell cycle arrest and apoptosis of hepatocytes. *Cell Death Dis* **9**: 762
7. Lebeaupin C, Vallee D, Hazari Y, Hetz C, Chevet E, Bailly-Maitre B (2018) Endoplasmic reticulum stress signalling and the pathogenesis of non-alcoholic fatty liver disease. *J Hepatol* **69**: 927-947
8. Mccullough KD, Martindale JI, klotz L-o, aw T-y, Holbrook NJ (2001) Gadd153 sensitizes cells to endoplasmic reticulum stress by down-regulating Bcl2 and perturbing the cellular redox state. *Mol Cell Biol* **21**: 1249-59
9. Chen BPC, Wolfgang CD, Hai T (1996) Analysis of ATF3, a transcription factor induced by physiological stresses and modulated by gadd153. *Mol Cell Biol* **16**: 1157–1168
10. Sylvester SL, Rhys CMJa, Luethy-Martindale JD, Holbrook NJ (1994) Induction of GADD153, a CCAAT/enhancer-binding protein (C/EBP)-related gene, during the acute phase response in rats. *J Biol Chem* **269**: 20119-20125
11. Puthalakath H, O'Reilly LA, Gunn P, Lee L, Kelly PN, Huntington ND, Peter D. Hughes, Michalak EM, McKimm-Breschkin J, Motoyama N*, et al.* (2007) ER stress triggers apoptosis by activating BH3-only protein Bim. *Cell* **129**: 1337-49
12. Uzi D, Barda L, Scaiewicz V, Mills M, Mueller T, Gonzalez-Rodriguez A, Valverde AM, Iwawaki T, Nahmias Y,

454 Xavier R*, et al.* (2013) CHOP is a critical regulator of acetaminophen-induced hepatotoxicity. *J Hepatol* **59**: 495-
455 503
456 13. Jiang H, Lin J, Su Z-Z, Goldstein NI, Fisher PB (1995) Subtraction hybridization identifies a novel melanoma
457 differentiation associated gene,mda7,modulated during human melanoma differentiation ,growth and
458 progression. *Oncogene* **11**: 2477-2486
459 14. Jiang H, Su Z-Z, Lin J, Young CSH, Goldstein NI, Fisher PB (1996) The melanoma differentiation-associated
460 gene mda-7 suppresses cancer cell growth. *Proc Natl Acad Sci USA* **93**: 9160-9165
461 15. Saeki T, Mhashilkar A, Swanson X, Zou-Yang XH, Sieger K, Kawabe S, Branch CD, Zumstein L, Meyn RE, Roth
462 JA*, et al.* (2002) Inhibition of human lung cancer growth following adenovirus-mediated mda-7 gene expression
463 in vivo. *Oncogene* **21**: 4558-66
464 16. Su Z-Z, Madireddi MT, Lin J, Young CSH, Kitada S, Reed JC, Goldstein NI, Fisher PB (1998) The cancer
465 growth suppressor gene mda-7 selectively induces apoptosis in human breast cancer cells and inhibits tumor
466 growth in nude mice. *Proc Natl Acad Sci USA* **95**: 14400-14405
467 17. Chada S, Sutton RB, Ekmekcioglu S, Ellerhorst J, Mumm JB, Leitner WW, Yang H-Y, Sahin AA, Hunt KK,
468 Fuson KL*, et al.* (2004) MDA-7/IL-24 is a unique cytokine-tumor suppressor in the IL-10 family. *Int*
469 *Immunopharmacol* **4**: 649-67
470 18. Sarkar D, Su Z-Z, Lebedeva IV, Sauane M, Gopalkrishnan RV, Valerie K, Dent P, Fisher PB (2002) MDA-7/(IL-
471 24) Mediates selective apoptosis in human melanoma cells by inducing the coordinated overexpression of the
472 GADD family of genes by means of p38 MAPK. *Proc Natl Acad Sci USA* **99**: 10054-10059
473 19. Gupta P, Walter MR, Su Z-Z, Lebedeva IV, Emdad L, Randolph A, Valerie K, DevanandSarkar, Fisher PB
474 (2006) BiP/GRP78 is an intracellular target for MDA-7/IL-24 induction of cancer-specific apoptosis. *Cancer Res*
475 **66**: 8182-91
476 20. Hasnain SZ, Borg DJ, Harcourt BE, Tong H, Sheng YH, Ng CP, Das I, Wang R, Chen AC-H, Loudovaris T*, et al.*
477 (2014) Glycemic control in diabetes is restored by therapeutic manipulation of cytokines that regulate beta cell
478 stress. *Nat Med* **20**: 1417-26
479 21. Yamamoto K, Yoshida H, Kokame K, Kaufman RJ, Mori K (2004) Differential contributions of ATF6 and XBP1
480 to the activation of endoplasmic reticulum stress-responsive cis-acting elements ERSE, UPRE and ERSE-II. *J*
481 *Biochem* **136**: 343-50
482 22. Hong F, Liu B, Wu BX, Morreall J, Roth B, Davies C, Sun S, Diehl JA, Li Z (2017) CNPY2 is a key initiator of the
483 PERK-CHOP pathway of the unfolded protein response. *Nat Struct Mol Biol* **24**: 834-839
484 23. Larson AM, Polson J, Fontana RJ, Davern TJ, Lalani E, Hynan LS, Reisch JS, Schiødt FV, Ostapowicz G, Shakil
485 AO*, et al.* (2005) Acetaminophen-induced acute liver failure: results of a United States multicenter, prospective
486 study. *Hepatology* **42**: 1364-72
487 24. Sidrauski C, Acosta-Alvear D, Khoutorsky A, Vedantham P, Gallagher, Hann B, Nader K, Walter P, Ang KK-H,
488 Wilson C*, et al.* (2013) Pharmacological brake-release of mRNA translation enhances cognitive memory. *eLife* **2**:
489 e00498
490 25. Wang M, Kaufman RJ (2014) The impact of the endoplasmic reticulum protein-folding environment on
491 cancer development. *Nat Rev Cancer* **14**: 581-97
492 26. Liu Y, Shao M, Wu Y, Yan C, Jiang S, Liu J, Dai J, Yang L, Li J, Jia W*, et al.* (2015) Role for the endoplasmic
493 reticulum stress sensor IRE1alpha in liver regenerative responses. *J Hepatol* **62**: 590-8
494 27. Han CY, Lim SW, Koo JH, Won Kim, Kim SG (2016) PHLDA3 overexpression in hepatocytes by endoplasmic
495 reticulum stress via IRE1-Xbp1s pathway expedites liver injury. *Gut* **65**: 1377-88
496 28. Fink EE, Moparthy S, Bagati A, Bianchi-Smiraglia A, Lipchick BC, Wolff DW, Roll MV, Wang J, Liu S, Bakin AV*,*
497 *et al.* (2018) XBP1-KLF9 Axis Acts as a Molecular Rheostat to Control the Transition from Adaptive to Cytotoxic

Unfolded Protein Response. *Cell Rep* **25**: 212-223 e4

29. Rao J, Yue S, Fu Y, Zhu J, Wang X, Busuttil RW, Kupiec-Weglinski JW, Lu L, Zhai Y (2014) ATF6 mediates a pro-inflammatory synergy between ER stress and TLR activation in the pathogenesis of liver ischemia-reperfusion injury. *Am J Transplant* **14**: 1552-61

30. Hotamisligil GkS (2010) Endoplasmic reticulum stress and the inflammatory basis of metabolic disease. *Cell* **140**: 900-17

31. Dent P, Yacoub A, Hamed HA, Park MA, Dash R, Bhutia SK, Sarkar D, Wang X-Y, Gupta P, Emdad L*, et al.* (2010) The development of MDA-7/IL-24 as a cancer therapeutic. *Pharmacol Ther* **128**: 375-84

32. Nakagawa H, Umemura A, Taniguchi K, Font-Burgada J, Dhar D, Ogata H, Zhong Z, Valasek MA, Seki E, Hidalgo J*, et al.* (2014) ER stress cooperates with hypernutrition to trigger TNF-dependent spontaneous HCC development. *Cancer Cell* **26**: 331-343

33. Werman A, Werman-Venkert R, White R, Lee J-K, Werman B, Krelin Y, Voronov E, Dinarello CA, Apte RN (2004) The precursor form of IL-1α is an intracrine proinflammatory activator of transcription. *Proc Natl Acad Sci USA* **101**: 2434–2439

34. Kandel-Kfir M, Almog T, Shaish A, Shlomai G, Anafi L, Avivi C, Barshack I, Grosskopf I, Harats D, Anafi YK (2015) Interleukin-1alpha deficiency attenuates endoplasmic reticulum stress-induced liver damage and CHOP expression in mice. *J Hepatol* **63**: 926-33

35. Sawa Y, Arima Y, Ogura H, Kitabayashi C, Jing-Jing Jiang, Fukushima T, Kamimura D, Hirano T, Murakami M (2009) Hepatic interleukin-7 expression regulates T cell responses. *Immunity* **30**: 447-57

36. Song M, Sandoval TA, Chae CS, Chopra S, Tan C, Rutkowski MR, Raundhal M, Chaurio RA, Payne KK, Konrad C*, et al.* (2018) IRE1alpha-XBP1 controls T cell function in ovarian cancer by regulating mitochondrial activity. *Nature* **562**: 423-428

Figure legends

Fig. 1 IL-24 expression in the ER stressed-mouse liver and hepatocytes. (A, B) WT mice were intraperitoneally injected with a single dose of CCL_4 (2ml/kg). (A) GRP78, IL-24 and CHOP protein levels in the liver tissues were evaluated by western blot at indicated time points. Results are normalized to β-actin. *n* = 3 independent experiments. (B) IL-24 and CHOP mRNA levels in the liver tissues were assessed by qRT-PCR at indicated time points. Results are normalized to β-actin. *n* = 3 biological replicates. (C, D) AML12 cells were exposed to Tm (5 μg/ml) for the indicated time period. IL-24 and CHOP levels were evaluated by western blot (C) and qRT-PCR (D) at indicated time points. *n* = 2 independent experiments (C) or 3 biological replicates (D). (E) AML12 cells were transfected with indicated siRNAs or negative control (NC) 24 h prior to Tm treatment. IL-24 protein levels at indicated time points were assessed by western blot. *n* = 3 independent experiments. (F) *Il24* promoter activity in AML12 cells expressing indicated siRNAs, as quantified using luciferase assay. *Renilla* luciferase activity was normalized to firefly activity and presented as relative luciferase activity. *n* = 3 biological replicates. Data are presented as means ± SEM. **P* < 0.05, ***P* < 0.01, ****P* < 0.001, *****P* < 0.0001. *P*-values were determined by two tailed *t*-test.

Fig. 2 The protective role of hepatocyte IL-24 in ER stress-induced cell death. Sex- and age-matched WT and IL-24-null mice were intraperitoneally injected with vehicle or CCL_4. (A) Mouse liver function was assessed by measuring serum ALT (left) and AST (right) levels. *n* = 5-8. (B) Mouse survival rate after CCL_4-treatment was determined via Log-rank (Mantel-Cox) analysis. *n* = 11-13. (C, D) H&E (C) and TUNEL (D) staining of the liver tissues from vehicle or CCL_4-treated mice. *n* = 5-8 mice. Scale bar, 100 μm. (E) Hepatocyte apoptosis after CCL_4-treatment was assessed by counting TUNEL positive cells. *n* = 5-8 mice. (F) AML12 cells were transfected with lentiviral vectors expressing IL-24-targeted

555 sgRNA (left, referred to as IL-24 KO) or IL-24 cDNA (right, referred to as IL-24 OE). An empty vector
556 was transfected as a negative control, respectively. Cell viability of indicated AML12 cells after Tm
557 stimulation was assessed by CCK8 assay. *n* = 3 biological replicates. Data are presented as means ±
558 SEM. **P* < 0.05, ***P* < 0.01, ****P* < 0.001. *P*-values were determined by two tailed *t*-test.

559 **Fig. 3 IL-24 deficiency facilitates PERK-eIF2α-CHOP UPR in hepatocyte.** (A, B) P-PERK, P-eIF2α,
560 CHOP and GRP78 protein levels in CCL_4-treated WT and IL-24 KO mice (A) and Tm-stimulated control
561 and IL-24 KO AML12 cells (B), as evaluated by western blot at indicated time points. *n* = 3 independent
562 experiments. (C) Immunohistological staining of P-eIF2α and CHOP in the liver tissues from CCL_4-
563 treated WT and IL-24 KO mice. *n* = 5-8 mice. Scale bar, 100 μm. Results were represented in median
564 integrated optical density (IOD) value. (D) GADD34, ATF4 and CHOP mRNA levels in the liver tissues
565 from vehicle or CCL_4-treated mice. *n* = 4-7 mice. (E) ATF4 and CHOP mRNA levels in indicated AML12
566 cells after Tm stimulation as assessed by qRT-PCR at indicated time points. (F) P-PERK and CHOP
567 protein levels in Tm-stimulated primary hepatocytes from WT and IL-24 KO mouse, as evaluated by
568 western blot. *n* = 3 independent experiments. Data are presented as means ± SEM. **P* < 0.05, ***P* <
569 0.01, ****P* < 0.001, *****P* < 0.0001. *P*-values were determined by two tailed *t*-test.

570 **Fig. 4 Hepatocyte IL-24 protects CHOP-executed cell death.** (A) AML12 cells were treated with
571 siCHOP or negative control (NC). Cell viability of indicated AML12 cells after Tm stimulation was
572 assessed by CCK8 assay. *n* = 3 biological replicates. (B) Serum ALT (upper) and AST (lower) levels in
573 WT, IL-24 KO, CHOP KO and IL-24/CHOP double KO (DKO) mice treated with CCL_4 for 24 h. *n* = 5-8
574 mice. (C) TUNEL staining (left) of the liver tissues from CCL_4-treated mice and quantification of TUNEL
575 positive cells (right). Scale bar, 100 μm. (D) IL-24 KO mice were intravenously injected with AAV
576 particles expressing an empty vector or mouse IL-24 8 weeks prior to CCL_4 administration. Liver injury

577 was assessed by serum ALT and AST levels. *n* = 4 mice. (E) IL-24, P-PERK, P-eIF2α, CHOP and
578 GRP78 protein levels in the liver tissues from CCL_4-exposed IL-24 KO mice with or without IL-24 re-
579 expression. *n* = 3 independent experiments. Data are presented as means ± SEM. **P* < 0.05, ***P* <
580 0.01, ****P* < 0.001, *****P* < 0.0001. *P*-values were determined by two tailed *t*-test.

581 **Fig. 5 Perturbation of PERK-eIF2α signaling compensates ER homeostasis upon IL-24 loss.** (A)
582 Indicated AML12 cells were pre-treated with 200 nM ISRIB or DMSO (Vehicle) 24 h prior to Tm
583 exposure. Cell viability of indicated AML12 cells after Tm stimulation was assessed by CCK8 assay. *n*
584 = 3 biological replicates. (B, C) WT and IL-24 KO mice were intraperitoneally injected with vehicle or
585 ISRIB (0.25 mg/kg) 60 min prior to CCL_4 administration. Liver injury was assessed by serum ALT and
586 AST levels (B) and TUNEL positive cell ratios (C). *n* = 5 mice. Scale bar, 100 μm. (D) Immunoblotting
587 of CHOP in the liver tissues from CCL_4-exposed mice with or without ISRIB treatment. *n* = 3 independent
588 experiments. (E) Immunoblotting of PERK in the precipitates obtained by immunoprecipitation of
589 endogenous GRP78 in indicated AML12 cells. *n* = 3 independent experiments. (F) IL-24 KO mice were
590 intravenously injected with AAV particles expressing an empty vector or mouse GRP78 8 weeks prior
591 to CCL_4 administration. Liver injury was assessed by serum ALT and AST levels. *n* = 5 mice. Data are
592 presented as means ± SEM. **P* < 0.05, ***P* < 0.01, ****P* < 0.001. *P*-values were determined by two
593 tailed *t*-test.

594 **Fig. 6 Hepatocyte IL-24 inversely correlates with liver function and CHOP expression in patients.**
595 (A) Immunohistological staining of IL-24 and CHOP in the liver tissues from healthy donors (*n* = 9),
596 cirrhosis (*n* = 9) and acute ALF (*n* = 22) patients. Scale bar, 100 μm. (B) Quantification of IL-24 protein
597 levels in (A), as represented in median integrated optical density (IOD) value. (C) IL-24 mRNA levels in
598 the human liver tissues indicated in (A), as assessed by qRT-PCR. Results are normalized to β-actin.

599 *n* = 9-22 patients. (D, E) Pearson correlation analysis between liver IL-24 protein level and serum ALT
600 level (D) or liver CHOP protein level (E). *n* = 22. (F) Immunoblotting of IL-24, P-eIF2α and CHOP in the
601 liver tissues from healthy donors and acute ALF patients. *n* = 9 patients. Data are presented as means
602 ± SEM. **P* < 0.05, ***P* < 0.01. *P*-values were determined by two tailed *t*-test.

603 **Fig. 7 Schematic model showing the interaction between cytoplasmic IL-24 and UPR modulators**
604 **within hepatocytes.** Hepatocyte ER stress engages sXBP1 for upregulating IL-24 transcription, which
605 in turn improves ER homeostasis and represses CHOP-mediated cell death by harnessing PERK-eIF2α
606 branch reaction.

607

608

609

610

611

612

613

614

615

616

617

618

619

620

Expanded View Figure Legends

Expanded View Fig. 1 Determination of the levels of IL-24 and UPR markers during hepatocyte stress. (A) Protein levels of IL-24 in different mouse tissues as assessed by western blot. *n* = 3 independent experiments. (B) Mouse liver function was evaluated by measuring serum ALT (left) and AST (right) levels 0-72 h post CCL_4 injection. *n* = 4. (C, D) ATF4, ATF6 and sXBP1 mRNA levels in CCL_4-treated mice (C) and Tm-stimulated AML12 cells (D), as evaluated by qRT-PCR at indicated time points. *n* = 3 biological replicates. Data are presented as means ± SEM. **P* < 0.05, ***P* < 0.01, ****P* < 0.001, *****P* < 0.0001. *P*-values were determined by two tailed *t*-test.

Expanded View Fig. 2 Hepatocyte XBP1 is essential for maintaining IL-24 transcription. (A) Alignment of responsive elements for CHOP (boxed) XBP1/ATF6 (red) found in the promoter region of *Il24*. The base positions of the consensus are indicated 5′→3′. Positions are relative to transcription initiation site. (B) AML12 cells were transfected with indicated siRNAs or negative control (NC) 24 h prior to Tm treatment. IL-24 mRNA levels at indicated time points were assessed by qRT-PCR. (C) *Il24* promoter activity in AML12 cells expressing siRNAs with or without Tm treatment (24 h), as quantified using luciferase assay. *Renilla* luciferase activity was normalized to firefly activity and presented as relative luciferase activity. *n* = 3 biological replicates. (D) Cell viability of Ctrl ($Xbp1^{f/w}$) and XBP1 KO ($Xbp1^{f/w}Alb^{Cre}$) mouse hepatocytes at indicated time points post Tm treatment was assessed by CCK8 assay. *n* = 3 independent experiments. (E, F) Protein (E) and mRNA (F) levels of IL-24 in Ctrl ($Xbp1^{f/w}$) and XBP1 KO ($Xbp1^{f/w}Alb^{Cre}$) mouse hepatocytes at indicated time points post Tm treatment. *n* = 3 independent experiments (E) or biological replicates (F). Data are presented as means ± SEM. **P* < 0.05, ***P* < 0.01, ****P* < 0.001, *****P* < 0.0001. *P*-values were determined by two tailed *t*-test.

Expanded View Fig. 3 IL-24 deficiency exacerbates ER stress-related liver injury. (A) PCNA

643 staining of the liver tissues from CCL_4-treated WT and KO mice. Hepatocyte proliferation after CCL_4-
644 treatment was assessed by counting PCNA positive cells. Scale bar, 100 μm. (B) IL6, TNFA and IL1A
645 mRNA levels in the liver tissues from vehicle or CCL_4-treated WT and IL-24 KO mice. *n* = 3 mice. (C-
646 E) Sex- and age-matched WT and IL-24-null mice were orally treated with vehicle or APAP (500 mg/kg).
647 (C) Mouse liver function was assessed by measuring serum ALT (left) and AST (right) levels. *n* = 5-8.
648 (D) Mouse survival rate after APAP-treatment was determined via Log-rank (Mantel-Cox) analysis. *n* =
649 9-10. (E) H&E and TUNEL staining of the liver tissues from APAP-treated WT and IL-24-null mice. *n* =
650 5-8. Scale bar, 100 μm. Data are presented as means ± SEM. **P* < 0.05, ***P* < 0.01, ****P* < 0.001. *P*-
651 values were determined by two tailed *t*-test.

652 **Expanded View Fig. 4 Extracellular IL-24 does not affect liver function.** Recombinant IL-24 (rIL-24)
653 (5 μg per mouse) was intraperitoneally treated one hour prior to CCL_4 administration. (A) Mouse liver
654 function was assessed by measuring serum ALT (left) and AST (right) levels. *n* = 6 mice. (B) H&E and
655 TUNEL staining of the liver tissues from Vehicle or rIL-24-pre-treated mice. Scale bar, 100 μm. (C) P-
656 PERK and CHOP protein levels in Vehicle or recombinant IL-24-pre-treated mice as evaluated by
657 western blot at indicated time points. *n* = 3 independent experiments. Data are presented as means ±
658 SEM. ***P* < 0.01, ****P* < 0.001. *P*-values were determined by two tailed *t*-test.

659 **Expanded View Fig. 5 Intrinsic IL-24 reduces Tm-induced hepatocyte apoptosis.** (A, B) Ratios of
660 early and late phases of apoptosis in AML12 cells expressing different levels of IL-24 with or without
661 Tm treatment, as evaluated by Annexin V-PI staining. Data are presented as means ± SEM. **P* < 0.05,
662 ****P* < 0.001, *****P* < 0.0001. *P*-values were determined by two tailed *t*-test.

663 **Expanded View Fig. 6 Hepatocyte IL-24 attenuates PERK-eIF2α-CHOP branch reaction.** (A) P-
664 PERK, P-eIF2α, CHOP and GRP78 protein levels in Tm-stimulated control and IL-24 OE AML12 cells,

as assessed by western blot. *n* = 3 independent experiments. (B) CHOP (upper) and ATF4 (lower) mRNA levels in Tm-stimulated control and IL-24 OE AML12 cells, as evaluated by by qRT-PCR at indicated time points. *n* = 3 biological replicates. (C) CHOP and GRP78 protein levels in APAP-treated WT and IL-24 KO mice, as evaluated by western blot at indicated time points. *n* = 3 independent experiments. (D) Bim, TRIB3 and Bcl2 mRNA levels in the liver tissues from vehicle or CCL_4-treated WT and IL-24 KO mice. *n* = 3 independent experiments. (E) P-IRE1α and ATF6 protein levels in CCL_4-treated WT and IL-24 KO mice, as evaluated by western blot at indicated time points. *n* = 3 independent experiments. (F) P-PERK and CHOP protein levels in CCL_4-treated AML12 cells, as evaluated by western blot at indicated time points. *n* = 3 independent experiments. Data are presented as means ± SEM. $^{**}P < 0.01$, $^{***}P < 0.001$. *P*-values were determined by two tailed *t*-test.

Expanded View Fig. 7 GRP78 compensates the anti-stress function of hepatocyte IL-24. (A) Immunoblotting of PERK in the precipitates obtained by immunoprecipitation of endogenous GRP78 in indicated AML12 cells. *n* = 3 independent experiments. (B) IL-24 KO mice were intravenously injected with AAV particles expressing an empty vector or mouse GRP78 8 weeks prior to CCL_4 administration. Liver injury was assessed by TUNEL positive cell ratios. *n* = 5 mice. Scale bar, 100 μm. (C) Immunoblotting of P-PERK and CHOP in the liver tissues from CCL_4-exposed IL-24 KO mice with or without GRP78 overexpression. *n* = 3 independent experiments. Data are presented as means ± SEM. $^{**}P < 0.01$. *P*-values were determined by two tailed *t*-test.

Fig. 1

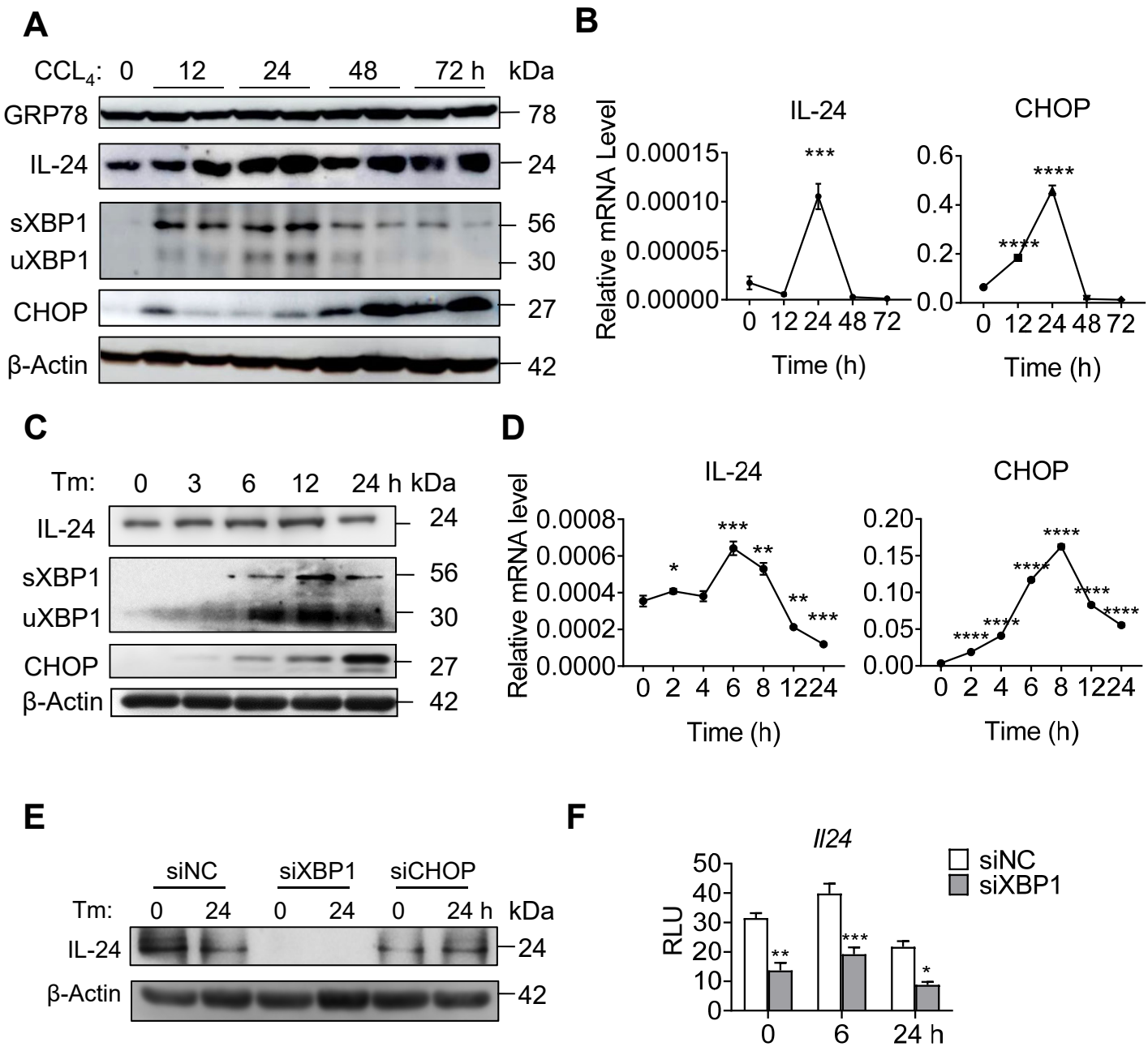

Fig. 2

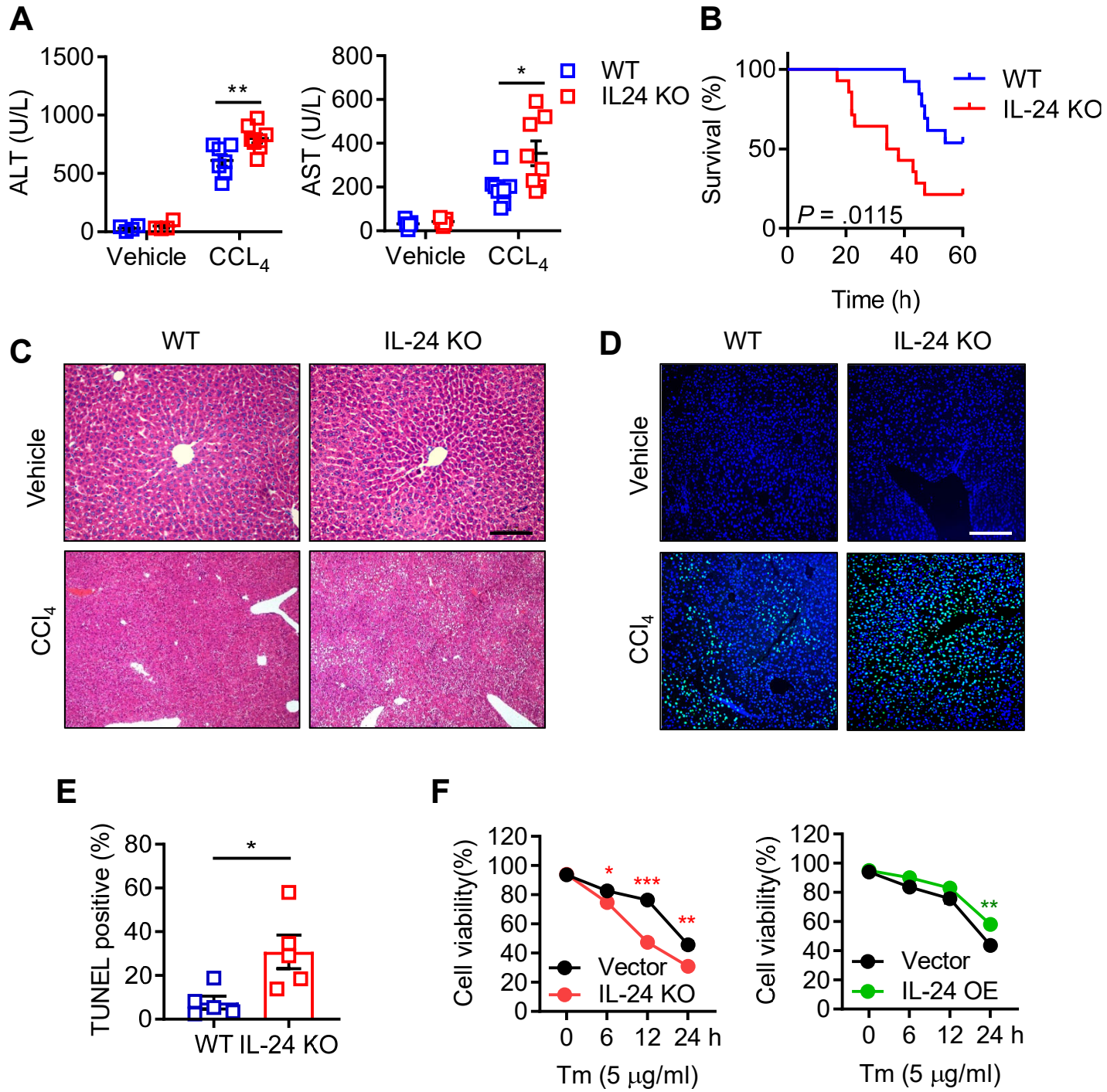

Fig. 3

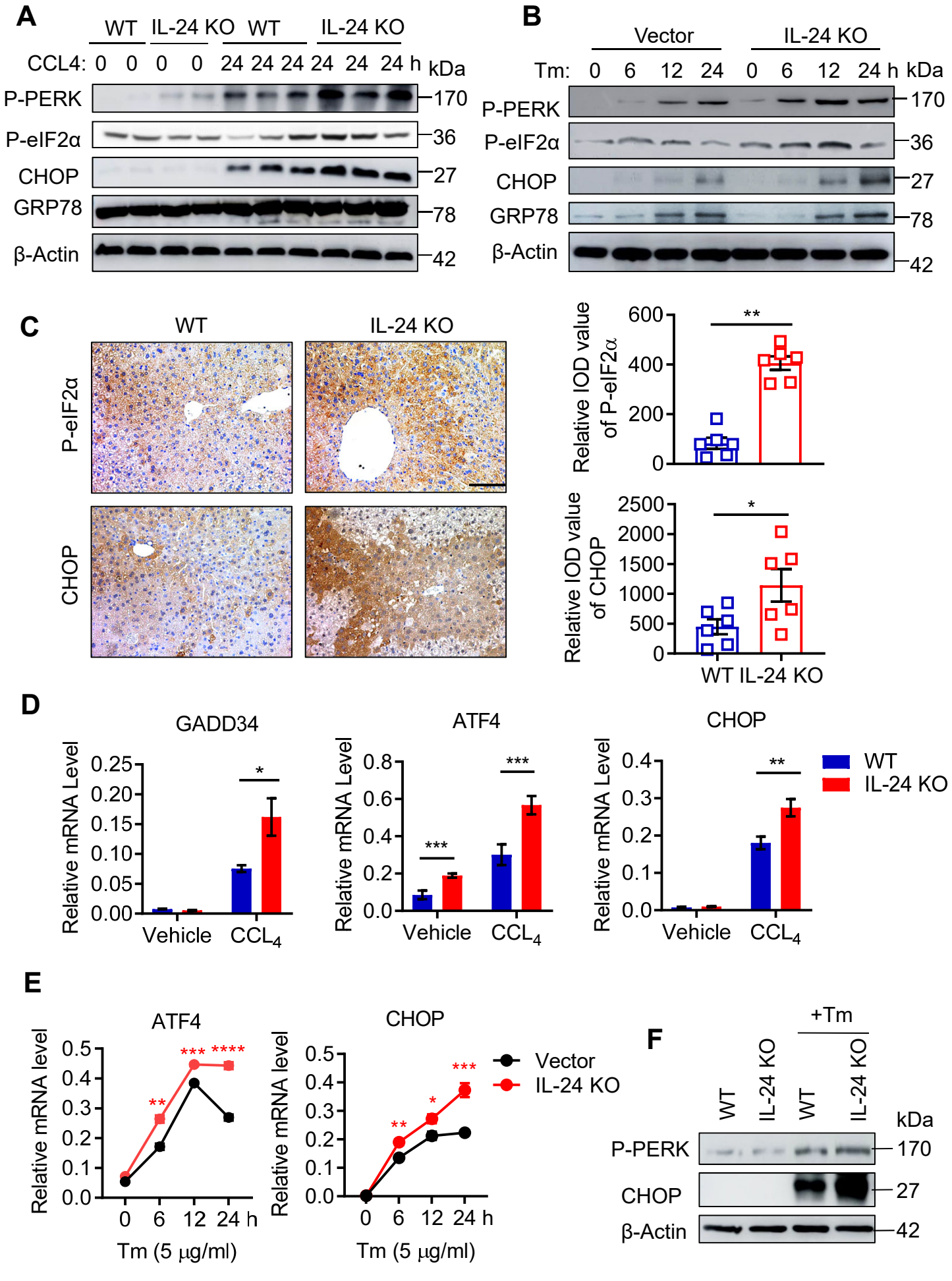

Fig. 4

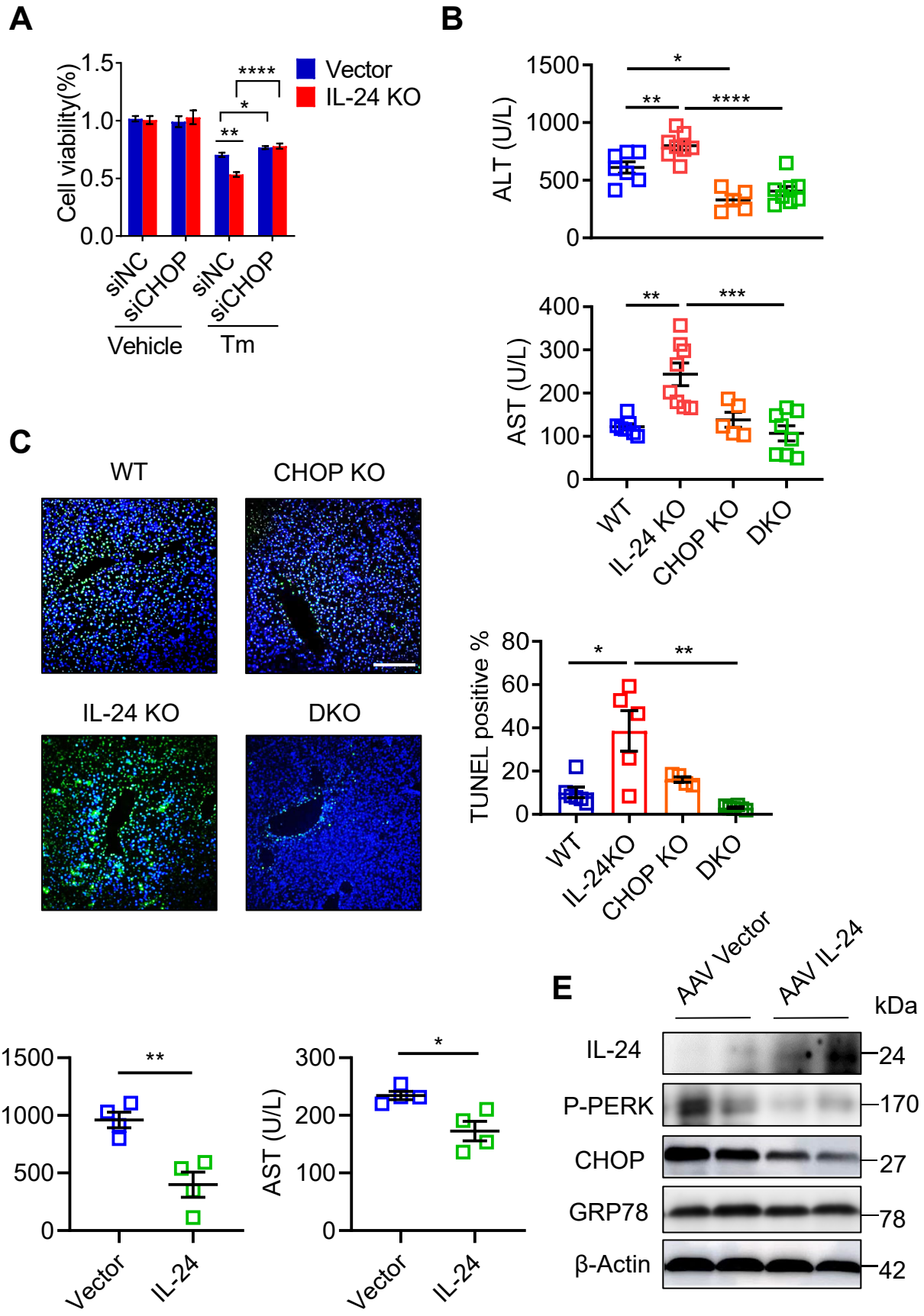

Fig. 5

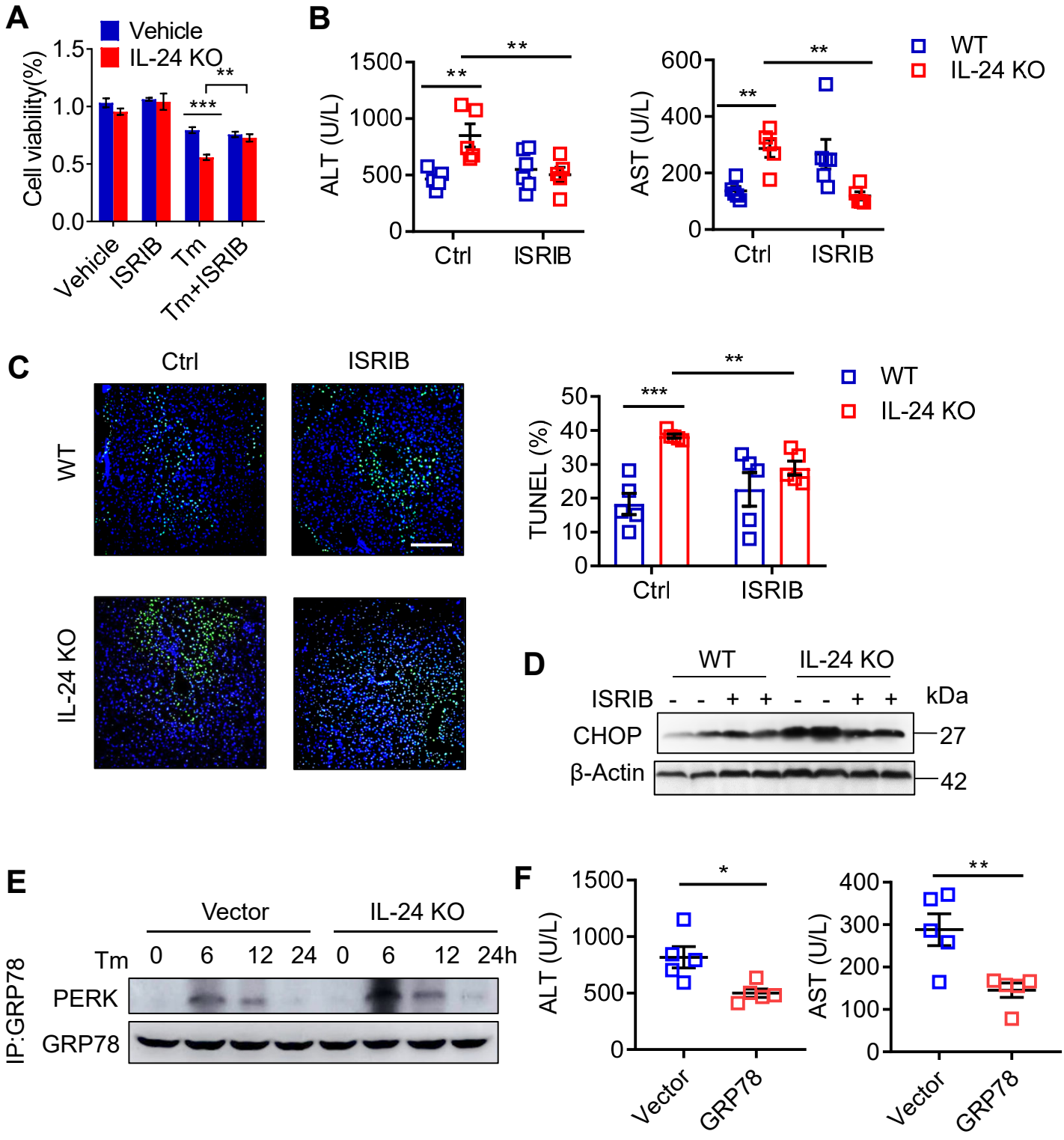

Fig. 6

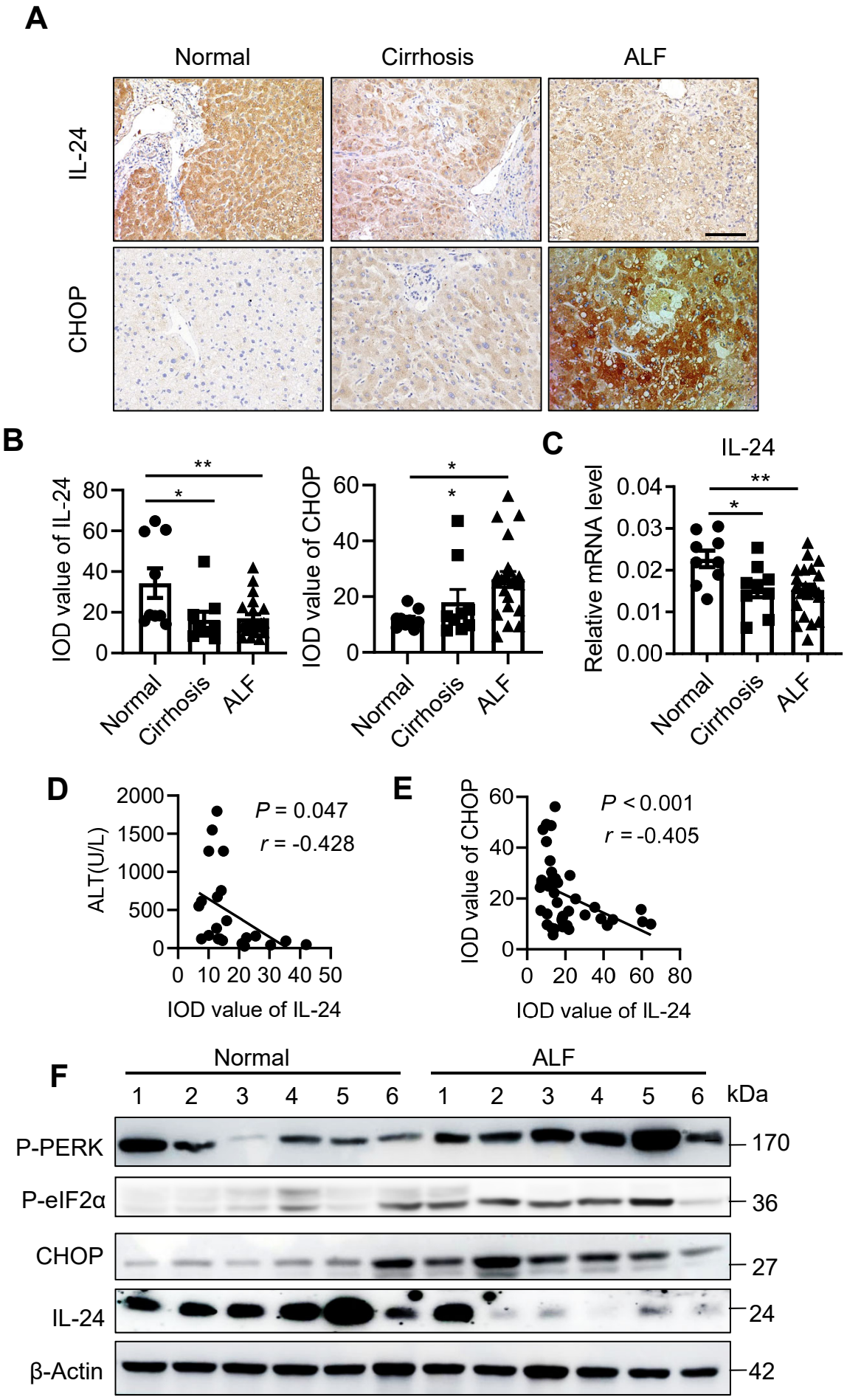

Fig. 7